Physica C 470 (2010) 2057–2060

Contents lists available at ScienceDirect

Physica C

journal homepage: www.elsevier.com/locate/physc

Theoretical investigation of the superconducting gaps in the Fe-based superconductors

Xiao-Shan Ye *

College of Physics Science and Technology, Yangzhou University, Yangzhou 225002, China

ARTICLE INFO

Article history:
Received 20 July 2010
Received in revised form 14 September 2010
Accepted 29 September 2010
Available online 8 October 2010

Keywords:
Fe-based compound
Superconducting gap
Phase variation

ABSTRACT

Based on an antiferromagnetic (AFM) spin fluctuation approximation, we study the superconducting gaps in Fe-based compound using two-band model. We find that our results are consistent with the previous work that concludes sign-reversal extended *s*-wave pairings between different Fermi surface sheets. The different superconducting gap magnitude around different Fermi surface sheets is probably due to the different density of states on them. This calculation can give insight to the recent angle-resolved photoemission (ARPES) experiments on these materials. To detect the phase variation of the superconducting gap over the Fermi surfaces, we propose a new method for measuring the particular wave vector phonon linewidth. In the case of the sign-reversal superconducting pairing, the linewidth shows continuities compared to the case of no phase variation.

The superconductivity found in Fe-based materials has attracted much attention [1–6]. Similar to cuprate superconductors, these materials are layered systems with a phase diagram where AFM phase is adjacent to the superconducting phase at low temperatures [7–9]. To understand the superconductivity of these materials it is essential to determine the superconducting pairing symmetry. Though extensive studies have been carried out, experimental results on the pairing symmetry in Fe-based superconductors are still controversial. Some experiments suggest the possible occurrence of conventional superconductivity [10–12]. Other suggest the possible occurrence of unconventional pairing [13–18]. Based on these experiments, several quite different theoretical proposals for its pairing symmetry such as the spin-singlet *s*-wave [19], the *d*-wave [20] and even the spin-triplet *p*-wave [21], have been put forward for different election interactions. Despite of the above exciting research progresses, it is still controversial for the gap symmetry. In particular, the recent ARPES experiments suggest that the superconducting gap magnitude are different on different Fermi surface sheets [22,23]. Some experiments suggest that the superconducting pairing state exhibits nodal behaviors [24,25]. So, there are still some experimental results to be explored: How to understand the different superconducting gap magnitude of the ARPES experiment. If the superconducting gap phase of the electron Fermi pockets is different from the holes, how can we detect it.

To begin with the two problems, we give three limitations for our consideration. First, though some groups propose that the electron–phonon interaction may be responsible for superconducting in the Fe-based materials, the calculated electron–phonon spectral function $\alpha^2F(\omega)$ and coupling λ for these compounds can not explain $T_c > 26$ K [26]. Therefore, we assume that the electron–phonon interaction in these materials is not the candidate accounting for the superconductivity. From the phase diagram we can see that the superconducting phase is adjacent to the AFM. We suggest that the superconductivity here is mediated by spin fluctuations. Second, the LDA band calculations indicate that two bands may be able to reproduce the main features of the four Fermi pockets. In this paper, we employ an effective two-band model Hamiltonian to explore the spin fluctuations and the superconductivity. Some groups use multiband to explore the superconducting property. We can extend our method readily to multiband of these compounds. Third, some argue the AFM spin fluctuations in these materials stemming from the interorbital Coulomb repulsion, the intraorbital Coulomb repulsion and the Hund's coupling. For simplicity we do not deal with these details. We will consider the intraorbital Coulomb repulsion influence on our results.

We start from an effective two-band model Hamiltonian [27,28]

$$H_0 = \sum_{k,\sigma} \Psi^+_\sigma(k)[(\varepsilon_+(k) - \mu)I + \varepsilon_-(k)\tau_3 + \varepsilon_{xy}(k)\tau_1]\Psi_\sigma(k) \quad (1)$$

with $\Psi^+_\sigma(k) = (d_{x\sigma}(k)d_{y\sigma}(k))$. Here τ_i are the usual Pauli matrices and $\varepsilon_\pm(k) = \frac{1}{2}[\varepsilon_x(k) \pm \varepsilon_y(k)]$, $\varepsilon_x(k) = -2t_1\cos k_x - 2t_2\cos k_y - 4t_3\cos k_x\cos k_y$, $\varepsilon_y(k) = -2t_2\cos k_x - 2t_1\cos k_y - 4t_3\cos k_x\cos k_y$, $\varepsilon_{xy}(k) =$

* Tel.: +86 51487975466.
E-mail address: xsye@yzu.edu.cn

0921-4534/$ - see front matter © 2010 Elsevier B.V. All rights reserved.
doi:10.1016/j.physc.2010.09.015

$-4t_4 \sin k_x \sin k_y$. Take the canonical transformation $\Psi_\sigma(k) = \sum_{\nu=\pm} u^r_\nu(k) a_{\nu\sigma}(k)$ with $u^x_+(k) = u^y_-(k) = \mathrm{sgn}(\varepsilon_{xy}(k))\sqrt{\frac{1}{2} + \frac{\varepsilon_-(k)}{2\sqrt{\varepsilon^2_-(k)+\varepsilon^2_{xy}(k)}}}$, $u^y_+(k) = -u^x_-(k) = \sqrt{\frac{1}{2} - \frac{\varepsilon_-(k)}{2\sqrt{\varepsilon^2_-(k)+\varepsilon^2_{xy}(k)}}}$, then we have $H_0 = \sum_{\nu=\pm,\sigma} E_\nu(k) a^+_{\nu\sigma}(k) a_{\nu\sigma}(k), E_\pm(k) = \varepsilon_+(k) \pm \sqrt{\varepsilon^2_-(k) + \varepsilon^2_{xy}(xy)} - \mu$.

In our calculations, we have used $t_1 = -1$, $t_2 = 1.3$, $t_3 = t_4 = -0.85$ and $\mu = 1.45$. In Fig. 1a, we plot the band structure of the two-band dispersion. Obviously, there exist two hole Fermi surfaces around $(0,0)$ and two electron Fermi surfaces around $(\pi,0)$. In Fig. 1b we show the Fermi surfaces for the same set of parameters.

Now we study the spin susceptibility for this tight-binding model. The orbital dependent spin susceptibility is defined as $\chi_{st}(\mathbf{q}, i\Omega) = \int_0^\beta d\tau e^{i\Omega\tau} < T_\tau S_s(-\mathbf{q},\tau) \cdot S_t(\mathbf{q},0) >$, here $s,t = 1,2$ label the orbital indices, and $S_s(\mathbf{q}) = \frac{1}{2}\sum_k \Psi^+_{s\alpha}(\mathbf{k}+\mathbf{q})\vec{\sigma}\Psi_{s\beta}(\mathbf{k})$ is the spin operator labeled by s. The physical spin susceptibility is given by $\chi_S(\mathbf{q}, i\Omega) = \sum_{s,t}\chi_{st}(\mathbf{q}, i\Omega)$. The one loop spin susceptibility we considered here can be obtained as $\chi_S(\mathbf{q}, i\Omega) = -\frac{T}{2N}\sum_{k,\omega_n} Tr[G(\mathbf{k}+\mathbf{q}, i\omega_n + i\Omega)G(\mathbf{k}, i\omega_n)]$, where the one electron Matsubara Green function is given by $G(\mathbf{k}, i\omega_n) = \frac{(i\omega_n - \varepsilon_+(\mathbf{k}))\widehat{I} - \varepsilon_-(\mathbf{k})\tau_3 - \varepsilon_{xy}(\mathbf{k})\tau_1}{(i\omega_n - E_+(\mathbf{k}))(i\omega_n - E_-(\mathbf{k}))}$. The static spin susceptibility $\chi_S(\mathbf{q},0)$ shows the largest value around $\mathbf{q} = (\pi,0)$, which suggests a transition to an antiferromagnetic order phase at some critical conditions. This is also in agreement with recent neutron scattering experiment. One can obtain the RPA spin susceptibility considering the electron–electron interorbital interaction V, intraorbital interaction U and the Hund coupling J, which is given by

$$\chi^{\mathrm{RPA}}_S(\mathbf{q}, i\Omega) = \chi_S(\mathbf{q}, i\Omega)(1 - \Gamma\chi_S(\mathbf{q}, i\Omega))^{-1}. \tag{2}$$

Where, the interaction vertex Γ has the following matrix form [28],

$$\hat{\Delta}_k = \begin{pmatrix} U & J/2 \\ J/2 & U \end{pmatrix}. \tag{3}$$

We find that the spin susceptibility is enhanced around $(\pi,0)$, but the structure of $\chi(\mathbf{q})$ remains qualitatively the same.

To discuss the nature of superconductivity, we will carry out the calculations by using the intraorbital interaction U. We have the effective pairing potential for the singlet channel [29],

$$V^s(\mathbf{q}, \omega_l) = U + \frac{3}{2}U^2\chi^{\mathrm{RPA}}_S(\mathbf{q}, \omega_l) - \frac{1}{2}U^2\chi_c(\mathbf{q}, \omega_l). \tag{4}$$

For $U > 0$, the spin fluctuation dominates over the charge fluctuation. We will ignore the charge fluctuation. Then, the superconducting gap functions are obtained by solving the linearized Éliashberg's equations,

$$\lambda\Delta_1(\mathbf{k}) = -\sum_{\mathbf{k}'} V^s(\mathbf{k}-\mathbf{k}', 0)\frac{\tanh(\beta E_2(\mathbf{k}')/2)}{2E_2(\mathbf{k}')}\Delta_2(\mathbf{k}')$$
$$\lambda\Delta_2(\mathbf{k}) = -\sum_{\mathbf{k}'} V^s(\mathbf{k}-\mathbf{k}', 0)\frac{\tanh(\beta E_1(\mathbf{k}')/2)}{2E_1(\mathbf{k}')}\Delta_1(\mathbf{k}') \tag{5}$$

with $\beta = 1/k_BT$. These equations have been shown to produce the $d_{x^2-y^2}$-wave pairing in the tetragonal lattice cuprates [30,31]. In the calculation, we decrease the temperature T gradually to search for the SC state, when the eigenvalue $\lambda = 1$ the SC state is reached. The calculations are carried out by dividing the extended Brillouin zone into 60×60 grids.

In Fig. 2, we present the self-consistent gap solutions. From the figure we can see that the two gaps are extended s-waves. There are three characters of the gaps: (a) The gaps have no nodes around all the Fermi surface sheets (the dot line in the figure are Fermi surfaces). (b) The signs of Δ_1 and Δ_2 is opposite. (c) The gap magnitude are different on different Fermi surfaces.

Next we give an explanation of the above results. The effective pairing potential V^s is determined mainly by the static spin susceptibility $\chi^{\mathrm{RPA}}_S(\mathbf{q}, \omega = 0)$. $\chi^{\mathrm{RPA}}_S(\mathbf{q}, \omega = 0)$ peaks near $(\pi,0)$, so the paring interaction in the spin-single channel is positive and has the largest intensity around the wave vector $\mathbf{q} = (\pi,0)$. From the Elishberger equations, we can see that the gap functions Δ have the largest magnitude and must change sign when $\mathbf{k}$ and $\mathbf{k}'$ are connected by $(\pi,0)$. Therefore they give rise to the sign reversal gap pairing. We also see that the magnitude of $\Delta_1(\mathbf{k})$ is different from $\Delta_2(\mathbf{k})$ from the figure. An explanation of this result is as follows. From the Elishberger equation we can see that the magnitude of the gap is proportional to the local density of states (DOS) of the system. This is more obvious in the conventional BCS theory. In our case, the DOS can be written as $N(\mathbf{k}) = 1/|\nabla_{\mathbf{k}}\varepsilon(\mathbf{k})|$ with $\varepsilon(\mathbf{k})$ the quasi-particle dispersion. From Fig. 1 we can see that the DOS near the electron Fermi surface is different from that of the holes. Thus, the magnitude of $\Delta_1(\mathbf{k})$ is different from that of $\Delta_2(\mathbf{k})$. Based on this discussion we speculate that the ratio of the magnitude of the two gaps would vary with the doping. The calculated result shown in Fig. 3 confirms our speculation. Next we give some remarks on our results with the ARPES experiments [22,23]. We observed that our results are not quite the same as ARPES. In the experiments, they found that the ratio of the magnitude of the gap is different not only between electron and hole Fermi pockets, but also between the hole Fermi pockets. We think that these discrepancies are not fundamental and can be reconciled without modifying the essential part of our results in the following reasons. First, we note that our result is sensitive to the DOS, so the discrepancies lie on the dispersion we used here. Second, in this weak-coupling approach we do not consider the renormalization of the

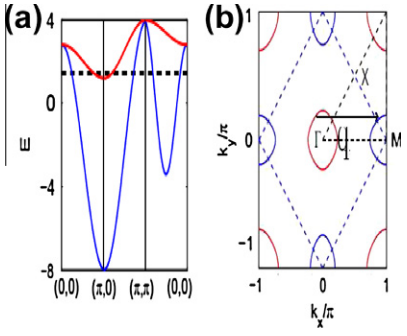

Fig. 1. (a) The band structure of the two-band model with $t_1 = -1$, $t_2 = 1.3$, $t_3 = t_4 = -0.85$, $\mu = 1.45$. The dashed line indicates the Fermi level. (b) The Fermi surface in the unfolded Brillouin zone. The line with an arrow denotes the nesting vector $q = (\pi,0)$ between the hole and electron Fermi pockets.

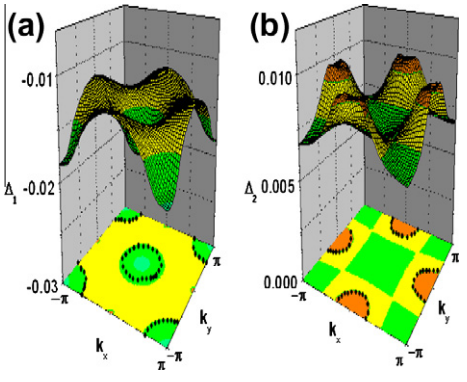

Fig. 2. Pairing gap functions in the unfolded Brillouin zone for $U = 3.0$ with $T = 0.01$ for $\mu = 1.45$. (a) Δ_1 for electron band. (b) Δ_2 for hole band.